Sulfur element achieves rapid and stable migration of Li^+ in oxide cathode

Lijuan Hou[a], Qi Liu[a,c]*, Daobin Mu[a], Li Li[a,b,c], Feng Wu[a,b,c], Renjie Chen[a,b,c]*

[a] Beijing Key Laboratory of Environment Science and Engineering, School of Material Science and Engineering, Beijing Institute of Technology, 100081, PR China

[b] Advanced Technology Research Institute, Beijing Institute of Technology, Jinan 250300, PR China

[c] Collaborative Innovation Center of Electric Vehicles in Beijing, Beijing, 100081, PR China

* Corresponding authors: liuqi985@bit.edu.cn, chenrj@bit.edu.cn

Experimental

Materials synthesis

Firstly, the $Ni_{0.90}Co_{0.05}Mn_{0.05}(OH)_2$ precursor material was obtained through coprecipitation method. Then the mixture of LiOH, $Ni_{0.90}Co_{0.05}Mn_{0.05}(OH)_2$, $(CH_3COO)_3Al$, TiO_2 and $Al_2(SO_4)_3$ was weighed according to the molar ratio of 1.08: 1: x: y: z, and put into a mortar with anhydrous ethanol for dispersion, the dried homogeneous powder sample was obtained by grinding in the mortar under an infrared lamp for about 30 min. Finally, the mixed powder was placed in a tube furnace under oxygen atmosphere for segmental calcination. The first stage was held at 500 °C for 5 h, the second stage was held at 700 °C for 10 h, where the heating rate was 5 °C min^{-1}, the oxygen airflow rate was 200 cubic foot per minute, and the cooling rate was 2 °C min^{-1}, and finally the calcination process was completed by dropping to room temperature, the calcined powder samples were collected and labeled as NCM (x=0, y=0, z=0), A-NCM (x=0.02, y=0, z=0), T-NCM (x=0, y=0.02, z=0), AT-NCM (x=0.01, y=0.01, z=0), ATS-NCM (x=0, y=0.01, z=0.005) respectively.

Materials characterizations

The crystalline phases of the NCM, A-NCM, T-NCM, AT-NCM and ATS-NCM powders were performed by X-ray diffraction (XRD) using Cu Kαradiation (X'pert PRO, PANalytical). The chemical composition of ATS-NCM was identified by inductively coupled plasma (ICP, OPIMA 8300, PerkinElmer). The surface information of the materials was characterized by X-ray photoelectron spectroscopy (XPS; Thermo Escalab 250Xi, USA). The microstructure and morphology of the materials were measured by a field-emission scanning electron microscopy (FESEM) (Regulus 8230) and energy dispersive spectrometer (EDS) mapping. The cross-sectional SEM samples of particles were prepared by a focused ion beam (FIB) technique (FEI Helios Nano Lab 450). The C 1s peak of a hydrocarbon located at 284.8 eV Binding Energy was act as calibration. Transmission electron microscopy (TEM) and high-resolution transmission electron microscopy (HRTEM) tests were conducted using a JEM-2100F transmission electron microscope. Atomic force microscopy (AFM) characterization was performed using a Bruker Dimensions ICON with a nano mirror V controller. Over 1000 points across the entire region was select to calculate the average Young's modulus within a specific range. Differential Scanning Calorimetry (DSC, TA

Q2000) was tested using delithiated electrode material charged to 4.6 V at a heating rate of 5 °C min^{-1} in an N_2 atmosphere within the temperature range of 100 to 300 °C, encapsulating 5 mg of the sample in a high-pressure stainless steel crucible and add approximately 50 wt% electrolyte.

Electrochemical measurements

CR2025 coin-type half-cells (or full battery) were employed to assess the electrochemical performances of the cathode materials. The homogeneous cathode slurry was obtained by the active materials, super P (as conductive) and polyvinylidene fluoride (PVDF, as binder) with an 8:1:1 wt ratio in N-methyl-1, 2-pyrrolidone (NMP) solvent. The cathode slurry was coated on the Al foil current collector and then casted into a diameter 11 mm tablet electrode with an active material mass loading of 2.5 ± 0.15 mg cm^{-2}. The argon-filled glovebox (H_2O < 0.1 ppm, O_2 < 0.1 ppm) was used to assemble the cells with Celgard 2400 as the separator, Li metal (graphite electrode with the active material mass loading of 2.5 ± 0.15 mg cm^{-2} in full battery) as the counter electrode, and 1 M $LiPF_6$ in ethyl carbonate/diethylene carbonate/dimetyl carbonate (EC/DEC/DMC = 1:1:1 in volume) as the electrolyte solution, respectively. Galvanostatic charge/discharge tests within the voltage range of 3.0–4.6 V at 30 ± 1 °C (Land CT2001A for coin-type cell) in the constant environmental chamber. For the current rate, the grams refer to the cathode active material for all coin-type half-cell and full-cell measurements. The cyclic voltammetry (CV) tests were performed in CHI660E electrochemical workstation with sweep rate of 0.1 mV s^{-1} and voltage window of 3.0–4.6 V. Electrochemical impedance spectroscopy (EIS, frequency range: 100,000–0.1 Hz, 3.0 V) was performed on a CHI6081D electrochemical system (Chen Hua).

In-situ XRD

In-situ XRD cell was employed with a Be window for X-ray penetration, the Al window acts as the current collector of the electrode. The fabrication process of the electrode for the in-situ XRD (BRUCKER D8 ADVANCE) measurement is same as that of the half-cell. The average loading of the electrode is approximately 4 mg cm^{-2}. The in-situ cell was aging for 24 h after assembled in glove box and charged/discharged at a rate of 0.05C. During the charging/discharging process, XRD measurement was repeated from 10°–90° with 20 min per

cycle.

Operando differential electrochemical mass spectrometry (DEMS)

The operation of DEMS is combined with GCD and CV measurements, consisting of a commercial quadrupole mass spectrometer (Hiden Analytical, model: HPR 40) and a Swagelok type DEMS cell (ECC Cell), with two glued capillary tubes used to purify the gas inlet and outlet. The flow rate of the purging gas is 0.5mL min-1. During the charging and discharging process, high-purity Ar is used as the working gas. In order to quantify the release of oxygen and other gases, a known constant Ar flow rate is used as the carrier gas. DEMS batteries are electrochemically controlled using a LAND cycle meter with a current density of 0.1C.

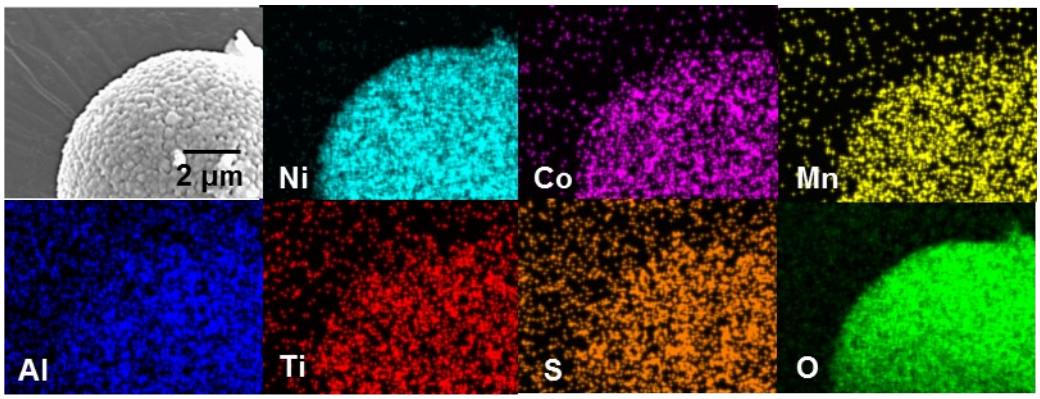

Figure S1 EDS mapping elemental analysis of ATS-NCM sample.

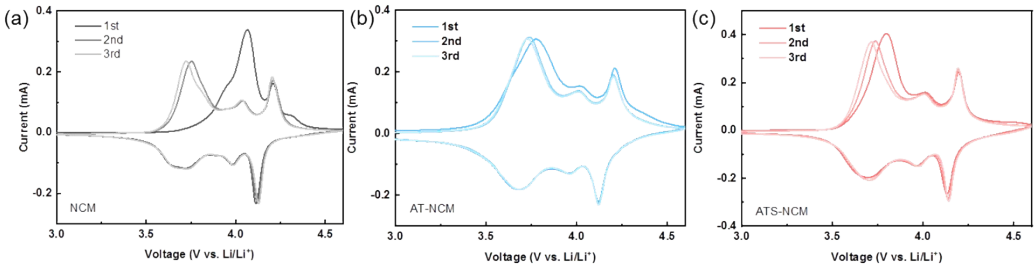

Figure S2 The CV for the first three cycles of NCM, AT-NCM and ATS-NCM electrodes.

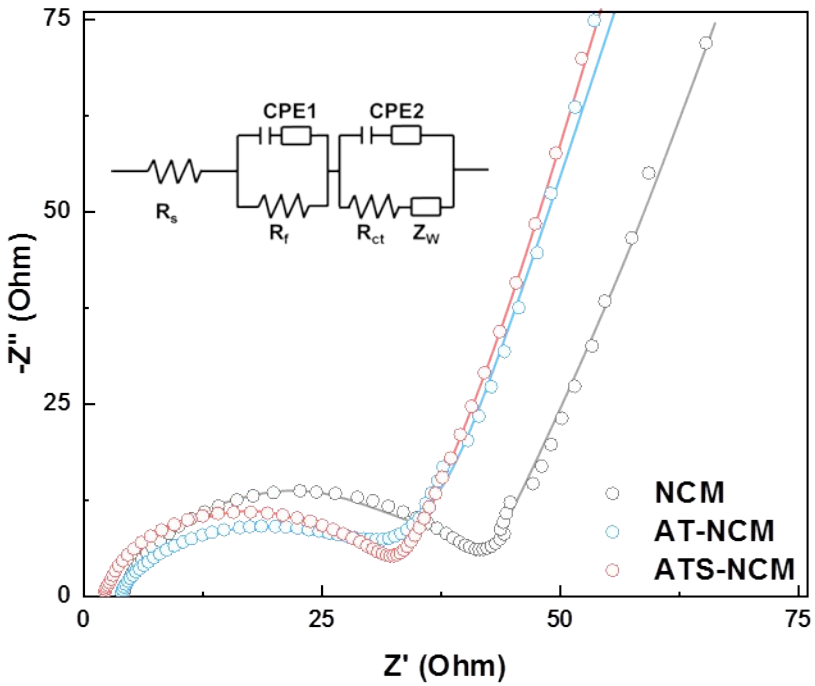

1

2 Figure S3 EIS Nyquist plots of NCM, AT-NCM and ATS-NCM.

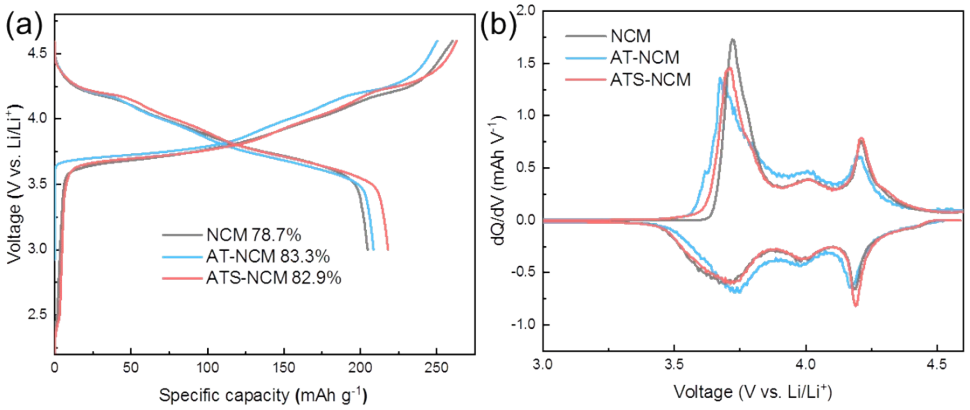

Figure S4 The first cycle charge discharge curves and corresponding dQ/dVq curves of NCM, AT-NCM and ATS-NCM cathodes.

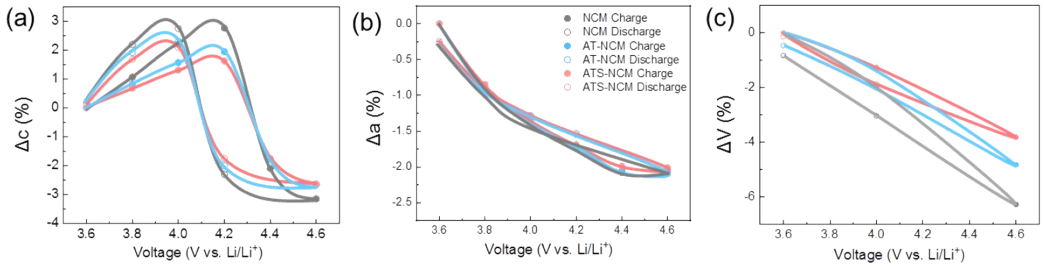

Figure S5 (a) a-lattice, (b) c-lattice and (c) volume parameter change rate of NCM, AT-NCM and ATS-NCM electrodes.

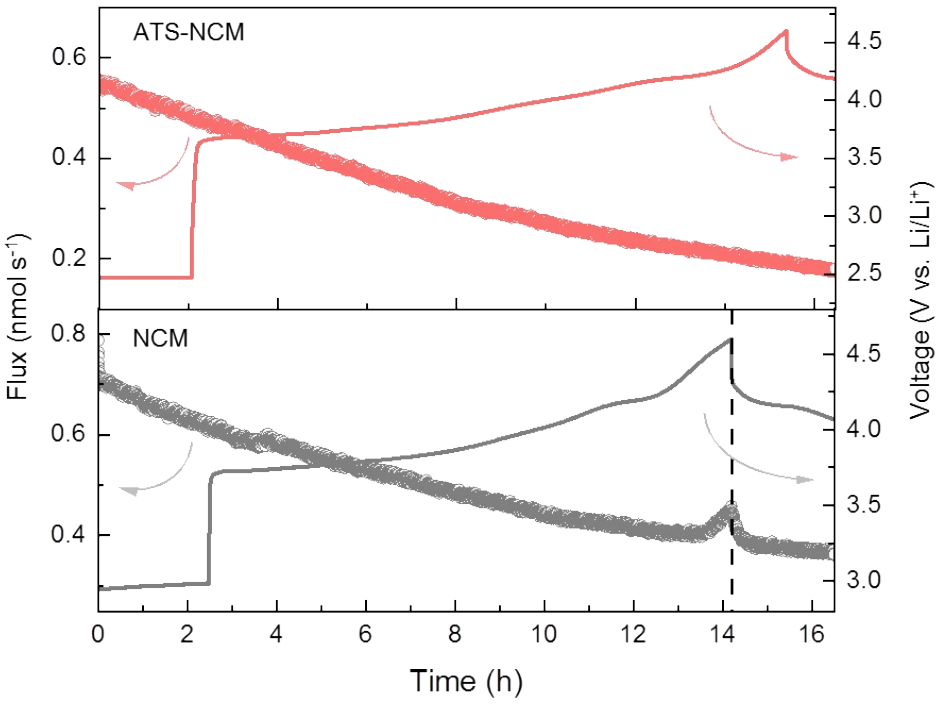

Figure S6 The DEMS curves of NCM and ATS-NCM electrodes during the initial cycle.

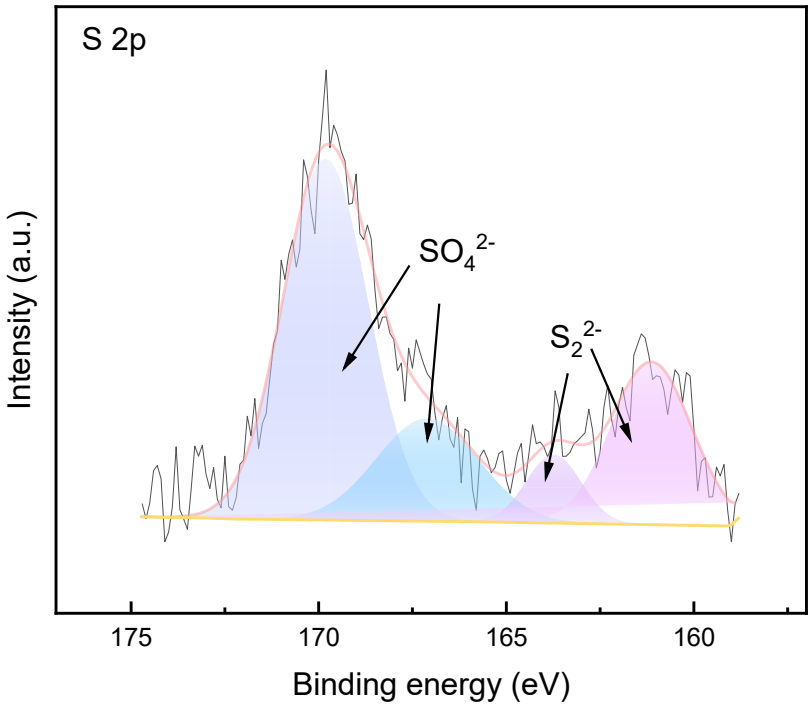

1

2 Figure S7 S 2p state for the ATS-NCM sample after cycling.

3

1 Table S1 EDS testing of element concentration in cross-section

Element	Line type	Apparent concentration	k ratio	Wt%	Wt%/Sigma	At%	Standard sample label
O	k-line	33.03	0.11116	18.69	0.26	45.56	SiO_2
Ni	k-line	80.47	0.80472	73.17	0.30	48.61	Ni
Co	k-line	5.04	0.05036	4.76	0.17	3.15	Co
Mn	k-line	3.23	0.03228	2.50	0.10	1.77	Mn
Al	k-line	0.14	0.00098	0.16	0.05	0.23	Al_2O_3
Ti	k-line	0.56	0.00564	0.51	0.07	0.41	Ti
S	k-line	0.24	0.00207	0.22	0.06	0.27	FeS_2
Total	/	/	/	100.00	/	100.00	/

2

3

Table S2 Comparison of calculated resistance of pure NCM, AT-NCM and ATS-NCM electrodes.

Matherials	R_f (Ω)	R_{ct} (Ω)
NCM	4.26	49.54
AT-NCM	3.79	42.07
ATS-NCM	2.26	37.56

Table S3 The molar ratio of each element in the before and after cycling ATS-NCM samples obtained from ICP testing.

ATS-NCM	Ni (%)	Co (%)	Mn (%)	Al (%)	Ti (%)	S (%)
Before cycling	88.8	5.1	3.3	0.6	0.8	1.4
After cycling	88.7	5.4	3.6	0.4	0.7	1.2